RSC Advances

PAPER

View Article Online
View Journal | View Issue

Cite this: *RSC Adv.*, 2024, **14**, 11775

PVDF/ZnO piezoelectric nanofibers designed for monitoring of internal micro-pressure

Geng Chang, Xuchao Pan,* Yu Hao, Wei Du, Siwei Wang, Yu Zhou, Jie Yang and Yong He

Organic piezoelectric materials are emerging as integral components in the development of advanced implantable self-powered sensors for the next generation. Despite their promising applications, a key limitation lies in their reduced mechanical force-to-electricity conversion efficiency. In this study, we present a breakthrough in the fabrication of soft poly(vinylidene fluoride) (PVDF) organic electrospun piezoelectric nanofibers (OEPNs) with exceptional piezoelectric performance achieved through the incorporation of zinc oxide nanorods (ZnO NR). The inclusion of ZnO NR proved instrumental in augmenting the nanocrystallization of PVDF organic electrospun piezoelectric nanofibers (OEPNs), leading to a highly efficient crystal phase transformation from the α phase to the β/γ phase, serving as superior piezoelectric working dipoles. The resulting PVDF/ZnO NR OEPNs exhibited unparalleled piezoelectric output voltage and current density, particularly noteworthy under a micro-pressure of 1 kPa and a low frequency of 1.5 Hz. Utilizing the obtained PVDF/ZnO NR OEPNs as the piezoelectric working element, we engineered a soft self-powered micro-pressure sensor. This sensor was implanted simultaneously on the cardiovascular walls of the heart and femoral artery in pigs. The sensor demonstrated precise monitoring and recording capabilities for micro-pressure changes during various physiological states, spanning from wakefulness to coma, euthanasia, and notably, the formation of cardiac thrombus. These findings underscore the immense potential of the implantable self-powered sensor for the assessment and diagnosis of pressure-related cardiovascular diseases, such as thrombus and atherosclerosis, during the postoperative recovery phase. This innovative technology offers valuable insights into the dynamic physiological states, paving the way for enhanced postoperative care and management of cardiovascular conditions.

Received 21st December 2023
Accepted 19th March 2024

DOI: 10.1039/d3ra08713a

rsc.li/rsc-advances

Introduction

Implanted micro-pressure biosensors hold significant promise for evaluating and diagnosing acute and chronic pressure-related diseases, encompassing cardiovascular diseases, brain injuries, hydrocephalus, glaucoma, and tumor regeneration.[1–7] However, their implementation has proven exceptionally challenging, primarily due to the limitations of conventional piezoelectric-based pressure sensors reported thus far. These sensors often exhibit suboptimal piezoelectric sensitivity and conversion efficiency, coupled with high biotoxicity, particularly under *in vivo* conditions.[8–10] In recent developments, organic piezoelectric materials have emerged as compelling candidates in the realms of bioelectronics and biomedicine. Their intrinsic flexibility, biocompatibility, and facile processability position them favorably for the advancement of implantable micro-pressure sensors.[11–15] Nevertheless, the current drawback lies in the limited piezoelectric performance of available organic materials, hampering their efficacy in converting internal micro-pressure into a discernible piezoelectric signal for biomedical applications *in vivo*.[16,17] Addressing this challenge necessitates the implementation of an effective strategy for fabricating ultrahigh-performance organic piezoelectric materials with exceptional biocompatibility. This strategic imperative stands as a pivotal factor in propelling the future development of implantable micro-pressure sensors.

Polyvinylidene fluoride (PVDF), recognized as a semi-crystalline polymer, predominantly exhibits piezoelectric properties in its β and γ phases, achievable through electrical polarization and physical stretching processes.[18–22] However, these post-treatments are often entangled with intricate processing protocols and yield limited piezoelectricity.[23–25] Notably, electrospinning has emerged as a favored technique to enhance the content of β and γ phases in organic piezoelectric materials. This is attributed to its ability to induce self-polarization and recrystallization within piezoelectric molecular structures in polymeric nanofibers (PNs), facilitated by high voltage application and rapid solvent evaporation.[26,27] The electrospinning method imparts exceptional flexibility and a distinctive nanofiber architecture to the resulting organic

School of Mechanical Engineering, Nanjing University of Science and Technology, Nanjing, 210094, China. E-mail: pxchxc@njust.edu.cn

electrospun piezoelectric nanofibers (OEPNs), ensuring their conformable adhesion to soft tissues and organs *in vivo* for real-time sensing of micro-pressure and deformation.[28–32] While OEPNs may appear to be ideal materials for the development of implantable self-powered pressure sensors, their current applications face significant challenges due to the inadequate sensitivity and intrinsic inefficiency in piezoelectric conversion. This limitation arises from the fact that internal pressures within organisms typically remain very weak (<1 kPa) and exhibit low frequencies (<1.5 Hz).

Efforts have been exerted to enhance the piezoelectric sensitivity and conversion efficiency of organic/inorganic electroactive polymer nanocomposites (OEPNs) by introducing nanofillers. This involves doping agents that establish molecular interactions with the $-CF_2$ groups of polyvinylidene fluoride (PVDF), inducing the formation of the β and γ phases. Examples of such nanofillers include metal nanoparticles (*e.g.*, Au), inorganic nanoparticles (*e.g.*, TiO_2 and barium titanate), functionalized multi-walled carbon nanotubes, graphene, and its derivatives.[33–35] These nanofillers have demonstrated a pronounced effect on enhancing the piezoelectric performance of OEPNs. For instance, in a study by Ji *et al.*, graphene oxide flakes doped PVDF OEPNs exhibited a piezoelectric constant 26% higher than that of pure PVDF OEPNs.[36] Another investigation by Ji *et al.* involved the preparation of flexible lead-free OEPNs based on BNT-ST ceramics and poly(vinylidene fluoride-trifluoroethylene) (PVDF-TrFE) copolymer. M. Wojtaś *et al.* have studied the dielectric and thermal stability of PVDF-TrFE copolymer doped with large amount of the graphene oxide (GO): 5, 10, 15, 20, 25%.[37,38] Well-arranged OEPNs in this study demonstrated an improved piezoelectric property (0.524 V cm^{-3}).[39] However, under micro-pressure (<1 kPa) and low frequency (<1.5 Hz) conditions, none of these materials displayed adequate piezoelectric performance for implantable self-powered pressure devices.[1–4]

In this study, we utilized nanoZnO as a nanofiller to enhance the piezoelectricity of PVDF OEPNs. NanoZnO was chosen for its high electromechanical coupling coefficient, physicochemical stability, and excellent biocompatible and antibacterial properties.[5] Considering the decisive role of nanoZnO's nanostructures on its electrochemical properties, three types of nanoZnO (nanoparticles and nanorods) were incorporated into PVDF OEPNs to investigate their impact on promoting the piezoelectric properties of PVDF OEPN. We conducted a comprehensive analysis of the morphology, crystal and chemical structure, as well as the electrochemical and piezoelectric performance of the resulting PVDF/ZnO OEPNs. Furthermore, we successfully designed and fabricated a soft self-powered pressure sensor using the PVDF/ZnO OEPNs as the piezoelectric working element. This sensor was implanted onto the cardiovascular walls of the heart and femoral artery to monitor and record changes in primitive blood pressure. The output piezoelectric signal from the soft sensor accurately and in real-time reflected fluctuations in blood pressure within the cardiovascular system. This was demonstrated as the pig underwent different pathological conditions, from waking to a comatose state, ultimately culminating in the euthanasia process. These findings not only pave the way for the development of high-performance organic piezoelectric materials for biomedical applications but also establish the implantable soft self-powered sensor as a versatile platform for a wide range of measurements related to internal micro-pressure.

Materials and method

Synthesis of PVDF/ZnO OEPNs

Schematic diagram of the electrospinning process for the fabrication of PVDF/ZnO OEPNs (Fig. 1). All materials were utilized without additional purification and were procured from reputable sources: PVDF (molecular weight = 53.4 kDa, Kun-Shan Hisense Electronic Co., Ltd, China), nanoZnO (Beijing Deke Island Gold Technology Co., Ltd), *N*,*N*-dimethylformamide (DMF, 99.5%, Sinopharm Chemical Reagent Co., Ltd, China), and acetone (99.5%, Shanghai Lingfeng Chemical Reagent Co., Ltd, China). To synthesize the PVDF/ZnO OEPNs, a 20% (wt/v) PVDF solution was prepared by dissolving PVDF in a mixture of DMF and acetone (volume ratio 3/2). Subsequently, nanoZnO was introduced into the solvent mixture, and the resulting solution was stirred for 12 hours to ensure uniform dispersion of ZnO. The solution was then injected into a spinneret (0.5 mm in diameter) using a microinjection pump at a rate of 1.0 ml h^{-1}. The spinneret was connected to a positive DC voltage of 18 kV, with the tip-to-collector distance maintained at 15 cm. The processing conditions included a temperature of 30 °C and a humidity level of 35%. The resultant PVDF/ZnO OEPNs were stored under vacuum conditions for subsequent investigations.

Chemical and morphology characterization

The examination of nanoZnO distribution within the organic electroactive polymer nanocomposites (OEPNs) and the morphological features of nanoZnO were scrutinized using a transmission electron microscope (TEM). The crystalline structure of these OEPNs was ascertained through the measurement of melting enthalpy *via* differential scanning calorimetry (DSC), employing the following formula:

$$X_c = \frac{\Delta H_f}{\Delta H_f^*}$$

wherein, X_c is the crystallinity of the sample. ΔH_f is the melting enthalpy of the sample. ΔH_f^* is the melting enthalpy of the sample of 100% crystallization, and the value is 104.5 J g^{-1}.

Piezoelectric properties

To assess the piezoelectric characteristics of the polyvinylidene fluoride/zinc oxide organic electrospun piezoelectric nanofibers (PVDF/ZnO OEPNs), a soft pressure sensor was meticulously devised and constructed. The OEPNs, measuring 20 mm × 20 mm with a thickness of 26 μm, were integrated by sandwiching them between two aluminum foils, firmly affixed using conductive adhesive. Copper wires served as the electrodes, and the sensor assembly was encapsulated within a packaging material film composed of

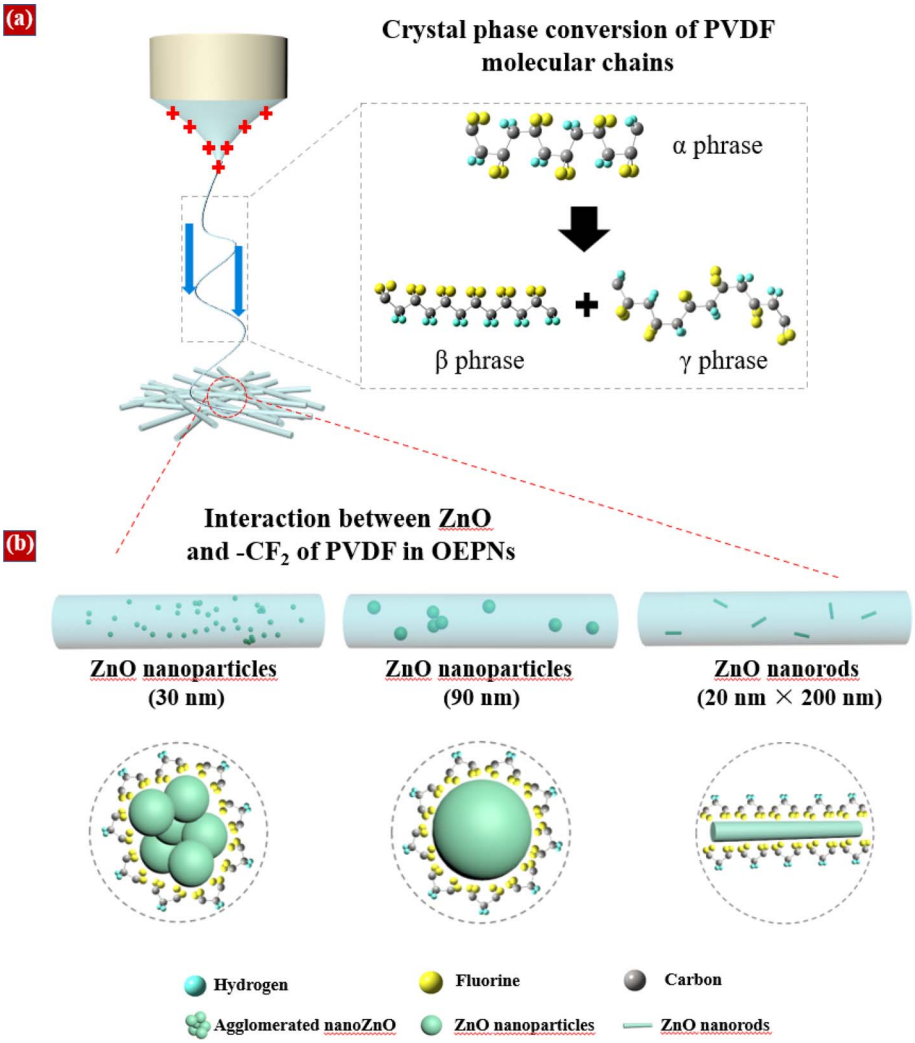

Fig. 1 Schematic diagram of the electrospinning process for the fabrication of PVDF/ZnO OEPNs. (a) Electrospinning and the crystal phase conversion in the PVDF/ZnO OEPNs; (b) effect of morphologies of nanoZnO on intermolecular interaction between $-CF_2$ of PVDF in the PVDF/ZnO OEPNs.

polyimide (PI) and polyethylene terephthalate (PET). Subsequently, a squeeze-release experimental setup was established to scrutinize the piezoelectric properties of the sensor. The experimental rig was actuated by an automotor operating at a frequency of approximately 1.5 Hz. Employing an electrochemical workstation (CHI 760e), the output piezoelectric voltage and current of the sensor were meticulously recorded and analyzed.

In vivo implantation and blood pressure monitoring

A male domestic pig weighing 80 kg underwent a 6 hour fasting period prior to the surgical procedure. The animal was anesthetized through an initial injection of ketamine (8 mg kg^{-1}, intramuscular) followed by propofol (1 mg kg^{-1}, intravenous). Anesthesia was sustained using 1.0% isoflurane. Subsequently, the right femoral artery and carotid artery were meticulously dissected, with careful separation of the artery and surrounding muscle tissue. Preceding implantation, the pressure sensor,

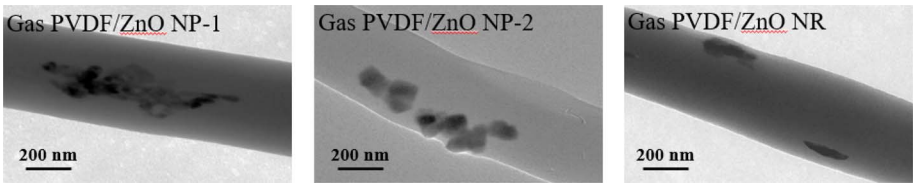

Fig. 2 TEM images of PVDF/ZnO OEPNs.

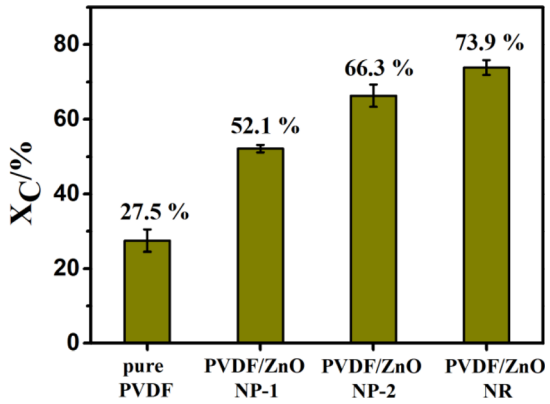

Fig. 3 Crystallinity of PVDF/ZnO OEPNs.

measuring 10 mm × 10 mm, underwent sterilization for one hour. The sensor was then implanted to envelop the surfaces of the right femoral and carotid arteries. Following implantation, the incision was sutured, and the animal was interfaced with an electrochemical workstation for continuous monitoring of voltage output. Throughout the procedure, the animal received compassionate care and was managed in strict adherence to the Institutional Animal Care and Use Committee (IACUC) approval protocol of the Animal Care Center at the Nanjing Military Region General Hospital.

Results and discussion

Fabrication and physicochemical characteristics of PVDF/ZnO OEPNs

In the course of electrospinning, three distinct nanoZnO variants exhibiting diverse morphologies, namely nanoparticles

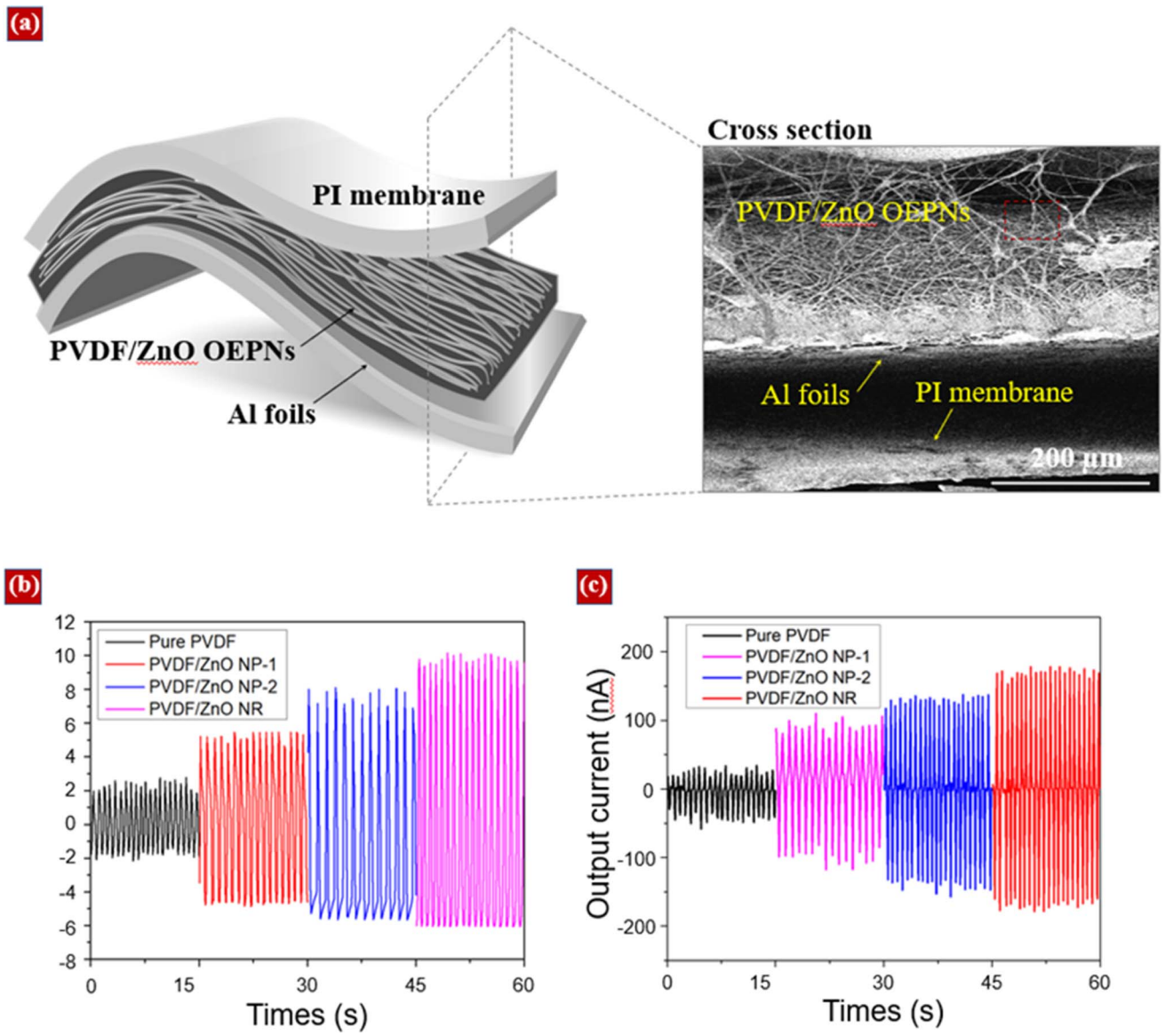

Fig. 4 Effect of nanoZnO on piezoelectric property of PVDF/ZnO OEPNs. (a) Schematic diagram of the PVDF/ZnO OEPNs based pressure sensor and the SEM image of the cross-sectional scan of the pressure sensor. (b) Output voltages and (c) current of the PVDF/ZnO OEPNs with the optimum doped ZnO concentrations.

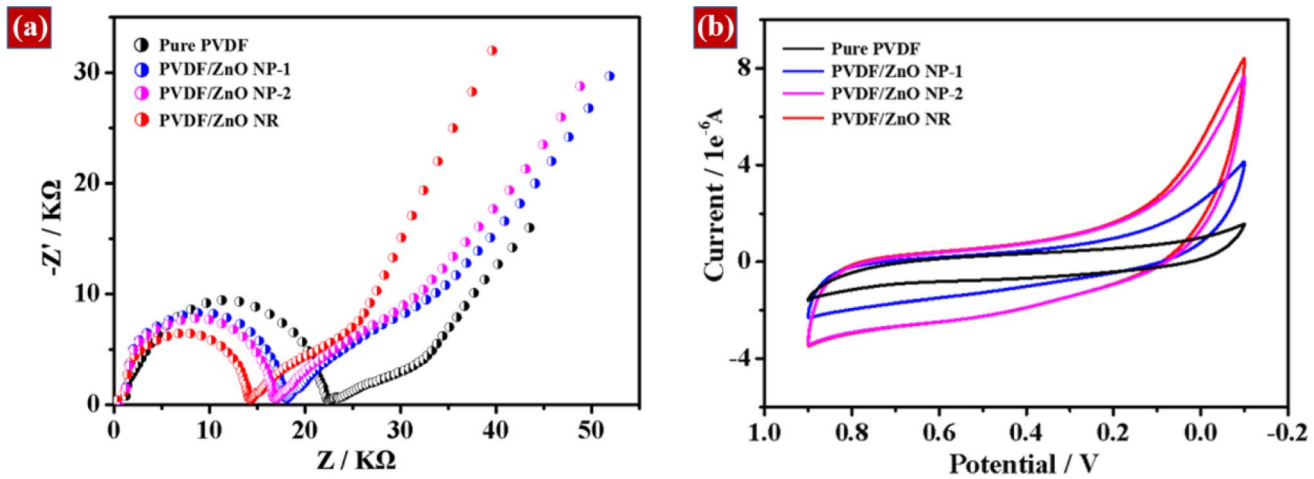

Fig. 5 Electrical properties of PVDF/ZnO OEPNs. (a) Impedance map (b) CV curve of different PVDF/ZnO OEPNs.

(average diameter: 30 ± 10 nm and 90 ± 10 nm) and nanorods (length: 200 ± 60 nm, diameter: 20 ± 8 nm), were incorporated into the organic electrospun polymer nanofibers (OEPNs). The successful integration of nanoZnO into the OEPNs during the electrospinning process is evidenced in Fig. 2c. TEM images further revealed the monodispersity of ZnO nanorods (ZnO NR) and nanoparticles with a diameter of 30 nm (ZnO NP-2). In contrast, ZnO nanoparticles with a diameter of 90 nm (ZnO NP-1) exhibited agglomeration, resulting in a size range of 200–350 nm due to the presence of abundant hydroxyl groups. The diameter distribution of the resulting PVDF/ZnO OEPNs ranged from 300 nm to 500 nm, as depicted in (Fig. 2 and 3). To achieve optimal levels of β/γ phase content in the OEPNs for each nanoZnO variant, the doping percentages were meticulously optimized. Ultimately, the most effective doping percentages for nanoZnO in the OEPNs were determined to be 1 wt% (ZnO nanoparticles of 30 nm), 0.25 wt% (ZnO nanoparticles of 90 nm), and 0.35 wt% (ZnO nanorods), denoted as PVDF/ZnO NP-1, PVDF/ZnO NP-2, and PVDF/ZnO NR, respectively.

The introduction of nanoZnO into the polymer matrix instigated a notably efficient phase conversion, leading to a marked enhancement in crystallinity, as depicted in Fig. 3. The initial crystallinity of pristine PVDF OEPNs, recorded at 27.5%, exhibited a significant surge to 52.1% upon incorporation of ZnO nanoparticles (PVDF/ZnO NP-1 OEPNs). Subsequent doping iterations with nanoZnO led to a continued escalation in crystallinity, reaching 66.3% for PVDF/ZnO NP-2 OEPNs and a peak of 73.9% for PVDF/ZnO NR OEPNs. This augmentation in the crystal structure of PVDF/ZnO OEPNs holds considerable implications for the improvement of their piezoelectric properties.

Piezoelectric and electrochemical properties of PVDF/ZnO OEPNs

To evaluate the piezoelectric attributes of the synthesized PVDF/ZnO organic/inorganic electrospun piezoelectric nanofibers (OEPNs), a compliant pressure sensor utilizing PVDF/ZnO OEPNs as the piezoelectric working element was meticulously devised and constructed, adopting a stratified "sandwich" configuration, as depicted in Fig. 4a. The output voltage and current of PVDF/ZnO nanorod (NR) OEPNs were systematically examined under low-pressure conditions (1 kPa) and a frequency of 1.5 Hz. Illustratively presented in Fig. 4b and c, the structural characteristics of the incorporated nanoZnO proved pivotal in enhancing the piezoelectric properties of the PVDF/ZnO OEPNs. The PVDF/ZnO NR OEPNs demonstrated optimal piezoelectric performance, surpassing that of ZnO nanoparticle (NP)-1 and NP-2. This superiority is attributed to the one-dimensional rod-like architecture of ZnO NR, inducing the formation of an orientational crystal interface between ZnO NR and the PVDF molecular chain. This interface proves instrumental in mitigating the damping effects of grain boundaries on piezoelectric electrons and augmenting the velocity of piezoelectric electronic transmission within the PVDF/ZnO OEPNs. Simultaneously, the proclivity of ZnO nanoparticles to agglomerate as depicted in (Fig. 2a) during the electrospinning process, owing to their elevated surface energy, hinders the regularity of the crystal structure within the OEPNs. This agglomeration obstructs the generation and transmission of piezoelectric electrons within the OEPNs. Consequently, achieving the optimal piezoelectric properties of the PVDF nanofibers (NFs) entails the judicious doping of ZnO nanorods during a conventional electrospinning process. The resulting PVDF/ZnO NR OEPNs were selected for further in-depth investigation.

The electrical characteristics of the polyvinylidene fluoride (PVDF) based organic-inorganic hybrid electroactive polymer nanocomposites (OEPNs) were systematically evaluated through a series of electrochemical analyses. The impedance spectroscopy results revealed a noteworthy disparity in the impedance values between PVDF/ZnO NR and PVDF/ZnO NR as illustrated in Fig. 5a, with the former exhibiting lower impedance. Cyclic voltammetry analyses demonstrated a consistent closed, smooth curve for all OEPNs, without the emergence of discernible redox peaks. This observation is indicative of the commendable electrochemical stability inherent in these OEPNs. Furthermore, the comparison of electronic storage and transmission capabilities, as depicted in Fig. 5b, affirmed that

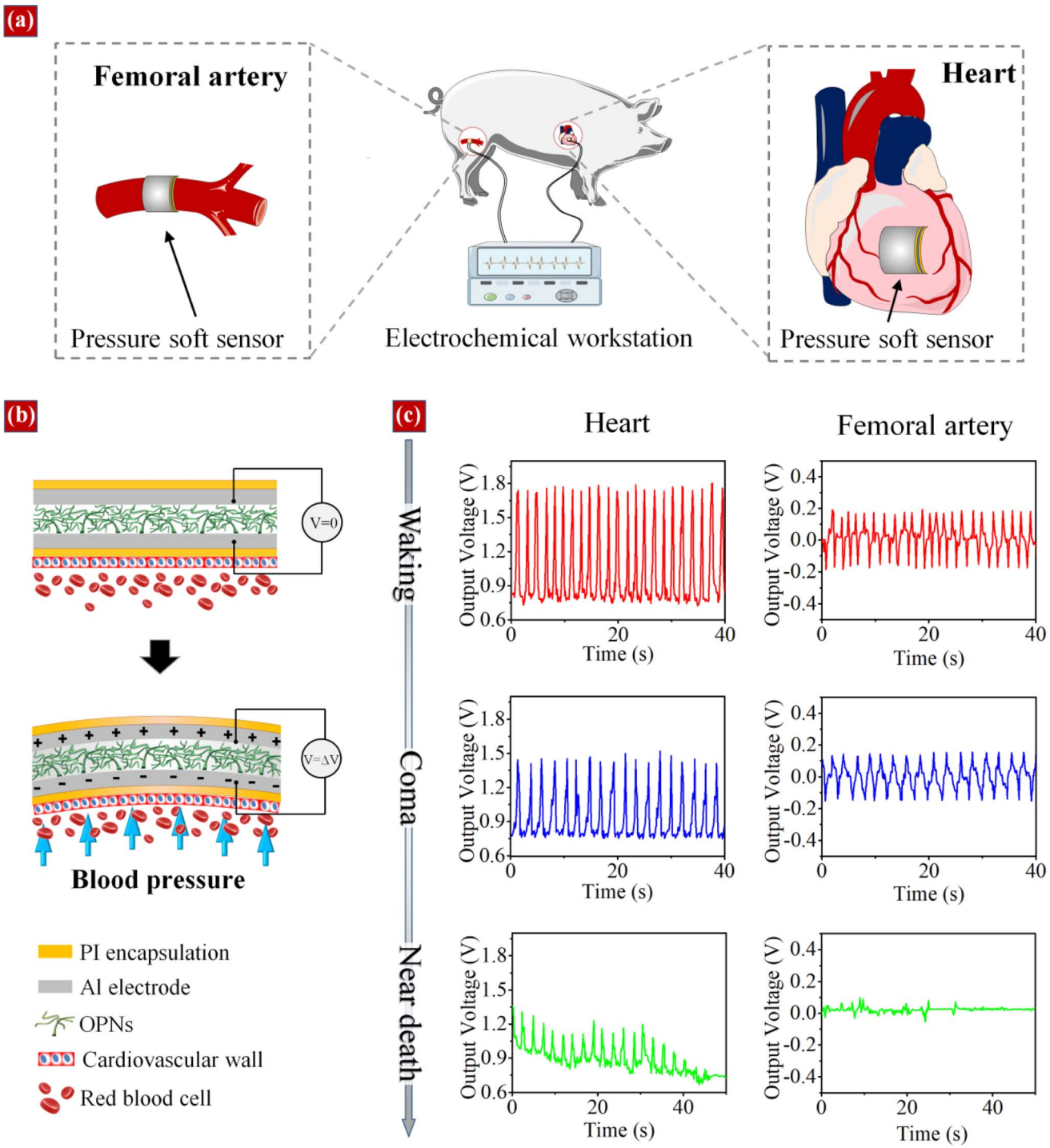

Fig. 6 Real-time monitoring of micropressure changes at the outside of cardiovascular wall *in vivo*. (a) Schematic of implantation of the sensor for recording micropressure changes. (b) Schematic of the working principle of the sensor for sensing micropressure changes caused by pulsation from the heart and femoral artery. (c) Output piezoelectric signals of the sensor when experimental pigs at different physiological states from waking to coma and near death.

PVDF/ZnO NR outperforms PVDF/ZnO NR in these aspects. These findings collectively underscore the superior electrical properties and electrochemical performance of PVDF/ZnO NR, suggesting enhanced electronic storage and transmission capabilities in comparison to their PVDF/ZnO NR counterparts.

Monitoring and recording of blood pressure changes at the outside of cardiovascular walls

To assess the pragmatic applicability of the PVDF/ZnO nanorod (NR) for *in vivo* blood pressure sensing, the PVDF/ZnO NR was set as the piezoelectric working element in the above soft

pressure sensor, which was covered with a thin PI membrane (thickness of 38 μm) to prevent the erosion of body fluids. Thus, the sensor has excellent flexibility to conformally attach onto the surface of the target organ to precisely sense their deformation and pressure changes, meanwhile, reduce organ damage caused by exogenous implantation. In this study, the soft pressure sensor was implanted into the femoral artery and heart of experimental pig by sticking procedure with bio-glue to monitor and record the internal blood pressure of the cardiovascular system at distal and proximal end respectively (Fig. 6a and b), because that the long-term and accurate internal blood pressure monitoring is still a key technical challenge for tracing of various pressure-related diseases such as vascular obstruction, hemangioma, hypertension, and so on. In addition, in order to test the sensitivity and accuracy of the soft sensor on the internal blood pressure changes under different physiological states, the experimental pig was firstly kept in waking state, and then injected with propofol and isoflurane to make it into coma state, finally the pig was euthanized by air embolism process.

Fig. 6c showed the piezoelectric output voltage of the soft sensor driven by the heart, when the pig was in the waking state, the output voltage was stable at about 0.93 ± 0.31 V. In consideration of the effective working area (10 mm × 10 mm, thickness: 26 μm) of the PVDF/ZnO NR in the soft sensor, the piezoelectric output voltage density of the sensor was 346.4 ± 115.2 V cm^{-3} under the cardiac blood pressure (left atrium, ~1.33 kPa). The value is significantly lower than the piezoelectric output voltage density of 1875 V cm^{-3} detected *in vitro*, which is because that the cardiac blood pressure cannot completely act on the sensor due to the soft tissue (including connective tissue, fat *e.g.*) surrounding the outside of the heart slowed down the attack from the blood pressure onto the sensor. However, the presence of these soft tissue does not affect the transmission of blood pressure change, thus the sensor sensed the cardiac blood pressure change sensitively. As shown in Fig. 6c, when the experimental pig was injected with anesthetic to become into coma state, the piezoelectric output voltage decreased into 0.51 ± 0.12 V immediately under a reduced cardiac blood pressure of ~1.13 kPa and stabilized at the level. Finally, when the experimental pig was applied with the euthanasia process, the piezoelectric output voltage gradually approaches zero (Fig. 6c). These results indicated that the implanted soft sensor has a high sensitivity to the changes in the cardiac blood pressure *in vivo*, which can semiquantitatively reflect the fluctuations in blood pressure as the experimental pig was at the different pathological condition.

Compared to heart, the femoral artery has a smaller working area (~4 mm × 10 mm) on the soft sensor, which led to a lower piezoelectric output voltage than that of the sensor implanted in the heart. As shown in Fig. 6c, the piezoelectric output voltage of the sensor on the femoral artery was about 0.36 ± 0.21 V and 0.15 ± 0.07 V when the experimental pig was at waking and coma state respectively. And the piezoelectric output voltage became into zero when the pig was death state. Clearly, the soft sensor monitored and recorded the fluctuation of blood pressure of the femoral artery caused by the different pathological condition of the pig, which was synchronous to the sensor implanted into the heart.

Obviously, these data collected *in vivo* demonstrated that the implanted PVDF/ZnO NR based soft sensor is sensitively enough to sense the internal blood pressure from distal (femoral artery) and proximal (heart) end of cardiovascular system, and the output voltage signals precisely reflected the fluctuation of blood pressure of experimental pig under different pathological condition. The global blood pressure monitoring and recording provide a promising strategy to build internal blood pressure map for diagnosis and prevention of cardiovascular-related diseases. In addition, the softness and ultrasensitivity of this implantable PVDF/ZnO NR based sensor enable it to be used not only in blood pressure monitoring but also other internal stress detection, such as intracranial pressure, intraocular pressure, renal pressure and so on. And compared to the traditional hard implantable pressure sensor, the soft pressure sensor is more suitable for long-term implantation to monitor internal chronic stress changes *in vivo* due to its biomechanical matching degree to organism and distinctive self-powered function. Therefore, the development of the implantable PVDF/ZnO NR based sensor provides a technical platform for extraction of internal pressure-related human health data.

Conclusions

Our investigation has successfully formulated an innovative methodology for fabricating highly responsive organic piezoelectric nanofibers using polyvinylidene fluoride (PVDF) doped with nanostructured zinc oxide (nanoZnO) through an electrospinning process. NanoZnO, functioning as a nucleating agent, played a pivotal role in orchestrating a proficient crystal phase transition from the α phase to the β/γ phases. The introduction of ZnO nanorods significantly augmented the piezoelectric properties. Employing the PVDF/ZnO nanorods as a transducer for converting mechanical stimuli into electrical signals, we engineered a pliable, self-powered pressure sensor. This sensor was precisely implanted into the femoral artery and heart of an experimental pig for the purpose of monitoring internal blood pressure. The implanted sensor exhibited exceptional sensitivity, furnishing real-time readings and accurately documenting fluctuations in blood pressure at both the distal and proximal ends of the cardiovascular system. Furthermore, the sensor adeptly discerned variations in blood pressure associated with a spectrum of pathological conditions, ranging from wakefulness to coma and ultimately euthanasia. The PVDF/ZnO nanorods, distinguished by their outstanding softness, biocompatibility, and piezoelectric characteristics, emerge as a highly auspicious candidate for intelligent pressure-responsive materials in internal pressure detection. This potential designates them as pivotal components for the diagnosis and monitoring of acute and chronic diseases correlated with internal pressure.

Data availability

Data will be made available on request.

Author contributions

XP was involved in methodology, investigation, data curation, writing and original draft. GC helped in writing—original draft, conceptualization. YH contributed to conceptualization, methodology and data curation. WD contributed to methodology and data curation. SW contributed to methodology. YZ contributed to investigation and data curation. JY contributed to writing-review & editing. YH contributed to writing-review & editing, supervision, resources and funding acquisition.

Conflicts of interest

The authors declare that they have no known competing financial interests or personal relationships that could have appeared to influence the work reported in this paper.

Acknowledgements

This work was made possible by the support of the Southern Xinjiang Key Industry Innovation and Development Support Project (Grant No. 2019DB011). The pig used in the experiments received humane care and were handled in accordance with IACUC approval protocol of the Animal Care Center at the Nanjing Jinling Hospital (SYXK 2019-0058).

References

1 B. Zhang, Q. Gao, W. Li, M. Zhu, H. Li, T. Cheng and Z. L. Wang, Alternating Magnetic Field-Enhanced Triboelectric Nanogenerator for Low-Speed Flow Energy Harvesting, *Adv. Funct. Mater.*, 2023, **33**, 2304839.

2 S. D. Mahapatra, P. C. Mohapatra, A. I. Aria, G. Christie, Y. K. Mishra, S. Hofmann and V. K. Thakur, Piezoelectric Materials for Energy Harvesting and Sensing Applications: Roadmap for Future Smart Materials, *Adv. Sci.*, 2021, **8**, 2100864.

3 Y. Dong, K. Zou, R. Liang and Z. Zhou, Review of BiScO3-PbTiO3 piezoelectric materials for high temperature applications: fundamental, progress, and perspective, *Prog. Mater. Sci.*, 2023, **132**, 101026.

4 J.-H. Lee, H.-J. Yoon, T. Y. Kim, M. K. Gupta, J. H. Lee, W. Seung, H. Ryu and S.-W. Kim, Energy Harvesting: Micropatterned P(VDF-TrFE) Film-Based Piezoelectric Nanogenerators for Highly Sensitive Self-Powered Pressure Sensors, *Adv. Funct. Mater.*, 2015, **25**, 3276.

5 X. Wang, Y. Huan, S. Ji, Y. Zhu, T. Wei and Z. Cheng, Ultra-high piezoelectric performance by rational tuning of heterovalent-ion doping in lead-free piezoelectric ceramics, *Nano Energy*, 2022, **101**, 107580.

6 M. Acosta, L. A. Schmitt, L. Molina-Luna, M. C. Scherrer, M. Brilz, K. G. Webber, M. Deluca, H.-J. Kleebe, J. Rödel and W. Donner, Core–Shell Lead–Free Piezoelectric Ceramics: Current Status and Advanced Characterization of the Bi1/2Na1/2TiO3–SrTiO3 System, *J. Am. Ceram. Soc.*, 2015, **98**, 3405–3422.

7 B. Ponraj, R. Bhimireddi and K. B. R. Varma, Effect of nano- and micron-sized K0.5Na0.5NbO3 fillers on the dielectric and piezoelectric properties of PVDF composites, *J. Adv. Ceram.*, 2016, **5**, 308–320.

8 S.-G. Lee, J. Y. Seo, J.-W. Lee, W. B. Park, K.-S. Sohn and M. Pyo, Composition-tuned lithium aluminosilicate as a new humidity-sensing ceramic material with high sensitivity, *Sens. Actuators, B*, 2021, **339**, 129928.

9 H. Khanbareh, K. de Boom, B. Schelen, R. B. N. Scharff, C. C. L. Wang, S. van der Zwaag and P. Groen, Large area and flexible micro-porous piezoelectric materials for soft robotic skin, *Sens. Actuators, A*, 2017, **55**, 554–562.

10 D. B. Deutz, N. T. Mascarenhas, J. B. J. Schelen, D. M. de Leeuw, S. van der Zwaag and P. Groen, Flexible Piezoelectric Touch Sensor by Alignment of Lead-Free Alkaline Niobate Microcubes in PDMS, *Adv. Funct. Mater.*, 2017, **27**, 1700728.

11 L. Lu, W. Ding, J. Liu and B. Yang, Flexible PVDF based piezoelectric nanogenerators, *Nano Energy*, 2020, **78**, 105251.

12 Z. A. Alhasssan, Y. S. Burezq, R. Nair and N. Shehata, Polyvinylidene Difluoride Piezoelectric Electrospun Nanofibers: Review in Synthesis, Fabrication, Characterizations, and Applications, *J. Nanomater.*, 2018, **2018**, 8164185.

13 S. K. Ghosh and D. Mandal, Synergistically enhanced piezoelectric output in highly aligned 1D polymer nanofibers integrated all-fiber nanogenerator for wearable nano-tactile sensor, *Nano Energy*, 2018, **53**, 245–257.

14 H. B. Lee, Y. W. Kim, J. Yoon, N. K. Lee and S.-H. Park, 3D customized and flexible tactile sensor using a piezoelectric nanofiber mat and sandwich-molded elastomer sheets, *Smart Mater. Struct.*, 2017, **26**, 045032.

15 Z. Liu, S. Li, J. Zhu, L. Mi and G. Zheng, Fabrication of β-Phase-Enriched PVDF Sheets for Self-Powered Piezoelectric Sensing, *ACS Appl. Mater. Interfaces*, 2022, **14**, 11854–11863.

16 S. Hao, C. Zhong, Y. Zhang, Y. Chen, L. Wang and L. Qin, Flexible 1-3 Piezoelectric Composites with Soft Embedded Conductive Interconnects for Underwater Acoustic Transducers, *ACS Appl. Electron. Mater.*, 2023, **5**, 2686–2695.

17 Z. Xu, M. Baniasadi, S. Moreno, J. Cai, M. Naraghi and M. Minary-Jolandan, Evolution of electromechanical and morphological properties of piezoelectric thin films with thermomechanical processing, *Polymer*, 2016, **106**, 62–71.

18 R. K. Singh, S. W. Lye and J. Miao, PVDF Nanofiber Sensor for Vibration Measurement in a String, *Sensors*, 2019, **19**, 3739.

19 L. Ruan, X. Yao, Y. Chang, L. Zhou, G. Qin and X. Zhang, Properties and Applications of the β Phase Poly(vinylidene fluoride), *Polymers*, 2018, **10**, 228.

20 S. Barrau, A. Ferri, A. Da Costa, J. Defebvin, S. Leroy, R. Desfeux and J.-M. Lefebvre, Nanoscale Investigations of α- and γ-Crystal Phases in PVDF-Based Nanocomposites, *ACS Appl. Mater. Interfaces*, 2018, **10**, 13092–13099.

21 X. Cai, T. Lei, D. Sun and L. Lin, A critical analysis of the α, β and γ phases in poly(vinylidene fluoride) using FTIR, *RSC Adv.*, 2017, **7**, 15382–15389.

22 A. Biswas, K. Henkel, D. Schmeißer and D. Mandal, Comparison of the thermal stability of the α, β and γ phases in poly(vinylidene fluoride) based on in situ thermal Fourier transform infrared spectroscopy, *Phase Transitions*, 2017, **90**, 1205–1213.

23 F. Khan, T. Kowalchik, S. Roundy and R. Warren, Stretching-induced phase transitions in barium titanate-poly(vinylidene fluoride) flexible composite piezoelectric films, *Scr. Mater.*, 2021, **193**, 64–70.

24 J. Yang, X. Yao and Z. Meng, Investigation of molecular mechanisms of polyvinylidene fluoride under the effects of temperature, electric poling, and mechanical stretching using molecular dynamics simulations, *Polymer*, 2022, **245**, 124691.

25 Q. Chi, G. Liu, C. Zhang, Y. Cui, X. Wang and Q. Lei, Microstructure and dielectric properties of BZT-BCT/PVDF nanocomposites, *Results Phys.*, 2018, **8**, 391–396.

26 A. Vicente, P. J. Rivero, J. F. Palacio and R. Rodríguez, The Role of the Fiber/Bead Hierarchical Microstructure on the Properties of PVDF Coatings Deposited by Electrospinning, *Polymers*, 2021, **13**, 464.

27 X. Wang, H. Zhu, G. W. Greene, J. Li, N. Iranipour, C. Garnier, J. Fang, M. Armand, M. Forsyth, J. M. Pringle and P. C. Howlett, Enhancement of ion dynamics in organic ionic plastic crystal/PVDF composite electrolytes prepared by co-electrospinning, *J. Mater. Chem. A*, 2016, **4**, 9873–9880.

28 C. Dong, Y. Fu, W. Zang, H. He, L. Xing and X. Xue, Appl. Self-powering/self-cleaning electronic-skin basing on PVDF/TiO2 nanofibers for actively detecting body motion and degrading organic pollutants, *Surf. Sci.*, 2017, **416**, 424–431.

29 Y. Yu, H. Sun, H. Orbay, F. Chen, C. G. England, W. Cai and X. Wang, Biocompatibility and in vivo operation of implantable mesoporous PVDF-based nanogenerators, *Nano Energy*, 2016, **27**, 275–281.

30 Ç. Defteralı, R. Verdejo, S. Majeed, A. Boschetti-de-Fierro, H. R. Méndez-Gómez, E. Díaz-Guerra, D. Fierro, K. Buhr, C. Abetz, R. Martínez-Murillo, D. Vuluga, M. Alexandre, J.-M. Thomassin, C. Detrembleur, C. Jérôme, V. Abetz, M. Á. López-Manchado and C. Vicario-Abejón, In Vitro Evaluation of Biocompatibility of Uncoated Thermally Reduced Graphene and Carbon Nanotube-Loaded PVDF Membranes with Adult Neural Stem Cell-Derived Neurons and Glia, *Front. Bioeng. Biotechnol.*, 2016, **4**, 94.

31 I. Tonazzini, E. Bystrenova, B. Chelli, P. Greco, D. De Leeuw and F. Biscarini, Human Neuronal SHSY5Y Cells on PVDF:PTrFE Copolymer Thin Films, *Adv. Eng. Mater.*, 2015, **17**, 1051–1056.

32 A. S. Motamedi, H. Mirzadeh, F. Hajiesmaeilbaigi, S. Bagheri-Khoulenjani and M. A. Shokrgozar, Piezoelectric electrospun nanocomposite comprising Au NPs/PVDF for nerve tissue engineering, *J. Biomed. Mater. Res.*, 2017, **105**, 1984–1993.

33 R. Yang, Y. Qin, C. Li, G. Zhu and Z. L. Wang, Converting Biomechanical Energy into Electricity by a Muscle-Movement-Driven Nanogenerator, *Nano Lett.*, 2009, **9**, 1201–1205.

34 K.-I. Park, S. Xu, Y. Liu, G.-T. Hwang, S.-J. L. Kang, Z. L. Wang and K. J. Lee, Piezoelectric BaTiO3 Thin Film Nanogenerator on Plastic Substrates, Effect of the top electrode on local piezoelectric and the ferroelectric response of PVDF thin films in PVDF/Au/Si and Ag/PVDF/Au/Si multilayers, *Nano Lett.*, 2010, **10**, 4939–4943.

35 M. S. Ravisankar, K. Pramod and R. B. Gangineni, Effect of the top electrode on local piezoelectric and the ferroelectric response of PVDF thin films in PVDF/Au/Si and Ag/PVDF/Au/Si multilayers, *Appl. Phys. Lett.*, 2023, **129**, 146.

36 S. H. Ji, J. H. Cho, Y. H. Jeong, J.-H. Paik, J. D. Yun and J. S. Yun, Flexible lead-free piezoelectric nanofiber composites based on BNT-ST and PVDF for frequency sensor applications, *Sens. Actuators, A*, 2016, **247**, 316–322.

37 M. Wojtaś, D. V. Karpinsky, M. V. Silibin, S. A. Gavrilov, A. V. Sysa and K. N. Nekludov, Dielectric properties of graphene oxide doped P(VDF-TrFE) films, *Polym. Test.*, 2017, **60**, 326–332.

38 M. Wojtaś, D. V. Karpinsky, M. V. Silibin, S. A. Gavrilov, A. V. Sysa, K. N. Nekludov and S. V. Dubkov, Pyroelectricity in graphene oxide doped P(VDF-TrFE) films, *Polym. Test.*, 2018, **71**, 296–300.

39 X. Liu, J. Ma, X. Wu, L. Lin and X. Wang, Polymeric Nanofibers with Ultrahigh Piezoelectricity via Self-Orientation of Nanocrystals, *ACS Nano*, 2017, 1901–1910.